

On the Spatial Distribution of High Velocity ^{26}Al Near the
Galactic Center

Steven J. Sturmer

Universities Space Research Association, 7501 Forbes Boulevard, Suite 206, Seabrook, MD
20706-2253

and

Laboratory for High Energy Astrophysics, Code 661, NASA, Goddard Space Flight Center,
Greenbelt, MD 20771

Received _____; accepted _____

ABSTRACT

We present results of simulations of the distribution of 1809 keV radiation from the decay of ^{26}Al in the Galaxy. Recent observations of this emission line using the Gamma Ray Imaging Spectrometer (GRIS) have indicated that the bulk of the ^{26}Al must have a velocity of $\sim 500 \text{ km s}^{-1}$ (Naya et al. 1996). We have previously shown that a velocity this large could be maintained over the 10^6 year lifetime of the ^{26}Al if it is trapped in dust grains that are reaccelerated periodically in the ISM (Sturmer & Naya 1999). Here we investigate whether a dust grain velocity of $\sim 500 \text{ km s}^{-1}$ will produce a distribution of 1809 keV emission in latitude that is consistent with the narrow distribution seen by COMPTEL. We find that dust grain velocities in the range 275 - 1000 km s^{-1} are able to reproduce the COMPTEL 1809 keV emission maps reconstructed using the Richardson-Lucy and Maximum Entropy image reconstruction methods while the emission map reconstructed using the Multiresolution Regularized Expectation Maximization algorithm is not well fit by any of our models. The ^{26}Al production rate that is needed to reproduce the observed 1809 keV intensity yields in a Galactic mass of ^{26}Al of $\sim 1.5 - 2 M_{\odot}$ which is in good agreement with both other observations and theoretical production rates.

Subject headings: gamma rays: observations — gamma rays: theory — nuclear reactions, nucleosynthesis, abundances — supernovae: general — supernova remnants

1. Introduction

In this paper we present a model to explain the spatial distribution of the Galactic emission at 1809 keV. The prediction (Ramaty & Lingenfelter 1977, Arnett 1977) and subsequent detection (Mahoney et al. 1984; Share et al. 1985)) of this nuclear decay line from the decay of ^{26}Al has been one of the major successes of theoretical nuclear astrophysics and gamma-ray astronomy. The main production mechanism for ^{26}Al is proton capture on ^{25}Mg and thus production sites must be proton and/or Mg rich. Proposed sites include core-collapse supernovae (SNe), Wolf-Rayet stars, asymptotic giant branch (AGB) stars, and classical novae (Clayton & Leising 1987; Prantzos & Diehl 1996; Diehl & Timmes 1997).

The COMPTEL gamma-ray telescope on the Compton Gamma-Ray Observatory (*CGRO*) has added greatly to our knowledge of this emission. It is an imaging Compton telescope with an angular resolution of 3.8° (FWHM) and an energy resolution of roughly 140 keV (FWHM) at 1809 keV (see e.g. Knödlseher 1997). Maps of the Galactic distribution of this radiation show that the emission is strongly concentrated to the Galactic plane (Diehl et al. 1997, 1995; Knödlseher et al. 1999a; Oberlack 1997) but the exact extent of the emission in Galactic latitude is not well constrained because of the the coarse angular resolution of the COMPTEL data (Knödlseher 1997). In order to better understand the source(s) of the ^{26}Al , the overall distribution of this emission has been compared with both those expected from simple source models such as exponential disks (Diehl et al. 1997; Knödlseher 1997) and emission maps at other wavelengths (Knödlseher et al. 1999b). Knödlseher et al. (1999b) found that the 1809 keV map was most similar the 53 GHz free-free emission map obtained using the *COBE* DMR (Bennett et al. 1992). This microwave emission is a tracer of ionized gass in the interstellar medium (ISM) and thus of massive stars in the Galaxy. This agreement between the distributions suggests that

sources associated with massive stars such as core-collapse supernovae and Wolf-Rayet stars are more likely to be the producers of ^{26}Al than either AGB stars and classical novae.

Studies of the kinematics of the ^{26}Al have been made possible through the use of high resolution germanium spectrometers. Naya et al. (1996) used the balloon-born Gamma Ray Imaging Spectrometer (GRIS) experiment to do such a study. They found that the intrinsic width of the 1809 keV line during Galactic Center transits was 5.4 (+1.4, -1.3) keV. The COMPTEL data does not have the energy resolution to confirm or contradict the GRIS line width results. This large width requires that the decaying ^{26}Al atoms have velocities of $\sim 540 \text{ km s}^{-1}$ which must be maintained over the $\sim 10^6$ year lifetime of the ^{26}Al . This is problematic since the Coulomb energy-loss timescale in the ISM for singly ionized atomic ^{26}Al is only ~ 500 years for a density of 1 cm^{-3} (see e.g. Sturmer & Naya 1999). Models to explain this observation have concentrated on binding the ^{26}Al into high-speed dust grains where the dominant energy loss mechanism in the ISM is thought to be direct collisions between grains and atoms (Drain & Salpeter 1979). There is mounting evidence that such high-velocity dust grains condense within the expanding ejecta of supernovae not long after the explosion. Early indications of this possibility came from analysis of the infrared (IR) light curves of extragalactic supernovae (Dwek et al. 1983) and analysis of isotopic abundances in meteorites (Clayton 1982). Final proof came from the optical and IR lightcurves of SN 1987A which show a dimming at optical wavelengths while the IR emissions brightened (see e.g. Dwek 1988; Dwek et al. 1992).

Chen et al. (1997) suggested a model in which the initial velocity of the dust grains is a consequence of the bulk motion of the ejecta during the early expansion phase. They found that while the energy-loss timescale of the grains was significantly longer than that of atomic ^{26}Al , the dust grains must still be injected into a very low density ($n_{\text{H}} < 10^{-2} \text{ cm}^{-3}$) environment if they are not to lose most of their energy prior to the decay of the ^{26}Al .

Ellison, Drury, & Meyer (1997) proposed that shock accelerating dust grains that contain ^{26}Al in the ISM may be an explanation for the GRIS observation. We have previously synthesized these concepts into a model for the production and maintenance of a high velocity distribution of ^{26}Al (Sturmer & Naya 1999). This model was able to explain the observed line widths given that the ^{26}Al is bound into fairly large dust grains ($\sim 10^{-5}$ cm), the ISM has a mean density near 0.2 cm^{-3} , and the ISM is permeated by SNR shocks with a mean separation of 100-200 pc. We found that the momentum of smaller dust grains ($\sim 10^{-6}$ cm) could not be maintained for the $\gtrsim 10^5$ year time periods between shock encounters.

The large velocity suggested by the GRIS measurement also has implications for the spatial distribution of the 1809 keV emission. As a rule of thumb, a particle moving at 1 km s^{-1} will travel ~ 1 pc in 10^6 years. Thus at the velocity required to explain the line width, the ^{26}Al will travel ~ 540 pc in its lifetime (assuming non-diffusive motion). This distance should not, however, be interpreted as the scale height of the ^{26}Al distribution. This would only be the case if all of the ^{26}Al were ejected perpendicular to the disk of the Galaxy in a pipe-like outflow. Here we examine whether the narrow latitudinal distribution of 1809 keV emission on the sky as measured by COMPTEL can be reconciled with the distribution expected from high velocity ^{26}Al assuming a more realistic radial outflow from the sources. We make no attempt to fit the longitudinal profile of the 1809 keV emission which has been examined in detail by Knodlseder et al.(1999b) and any analysis requires the use of complicated source models. In Section 2 of this paper we discuss our model for calculating the Galactic distribution of ^{26}Al and the 1809 keV sky map. In Section 3 we compare the results of our model calculations with the COMPTEL results and discuss what contribution the upcoming *INTEGRAL* mission can make to the field.

2. Model

We have produced a simple model to calculate the distribution of the 1809 keV emission which has three parts, ^{26}Al production, ^{26}Al transport, and sky map generation. In this model the ^{26}Al is generated within the Galaxy with a production function

$$\frac{dP}{dV_s dt}(\rho_s, z_s) = \epsilon_o f(\rho_s) g(z_s), \quad (1)$$

where we have assumed that it is a separable function of the cylindrical coordinates ρ_s and z_s (azimuthal symmetry is assumed). In this work we will assume for simplicity that most of the ^{26}Al in the Galaxy is produced in Type II SNe. Stecker & Jones (1977) suggested a functional form for the SNR surface density

$$f(\rho_s) = \left(\frac{\rho_s}{\rho_\odot}\right)^\alpha \exp\left(-\beta \frac{\rho_s - \rho_\odot}{\rho_\odot}\right), \quad (2)$$

where ρ_\odot is the distance from the Sun to the Galactic Center which we take to be 8.5 kpc (we assume that $z_\odot = 0$ kpc). Case & Bhattacharya (1998) have re-calibrated the $\Sigma - D$ relationship for Galactic SNRs and have used this result to derive the values $\alpha = 2.00 \pm 0.67$ and $\beta = 3.53 \pm 0.77$ which we use here. Using these parameter values, the surface density rises from zero at $\rho_s = 0$ kpc to a peak at $\rho_s = 4.8$ kpc from which point the density decreases (see Figure 1).

The distribution of SNe perpendicular to the disk is generally assumed to be that of an exponential disk

$$g(z_s) = \exp(-|z_s|/z_o). \quad (3)$$

The value for the supernova scale height that we use in our calculations is $z_o = 90$ pc, assuming it is the same as for massive stars ($M \gtrsim 3M_\odot$) (Miller & Scalo 1977; Bahcall & Soneira 1980; Ferrière 1993). We will treat ϵ_o in equation (1) as a free parameter to

adjust the normalization of the emission to fit the observations. We will then calculate the Galactic mass of ^{26}Al using this normalization.

Once produced, we assume the ^{26}Al flows radially away from the source locations (ρ_s, ϕ_s, z_s) at constant velocity v_o . During the radial outflow, the ^{26}Al decays with a 10^6 year time constant, τ_o . The density of ^{26}Al at position (ρ, ϕ, z) due to production in volume dV_s about the position (ρ_s, ϕ_s, z_s) is given by

$$dn(\rho, \phi, z, \rho_s, \phi_s, z_s) = \frac{dP}{dV_s dt} \exp(-d/v_o \tau_o) \frac{dV_s}{4\pi d^2 v_o}. \quad (4)$$

where $d = d(\rho, \phi, z, \rho_s, \phi_s, z_s)$ is the distance from the source location to the reference point (ρ, ϕ, z) . The three terms in equation (4) represent the production, decay, and outflow of the ^{26}Al . The total density at position (ρ, ϕ, z) due to emission throughout the Galaxy is just

$$N(\rho, \phi, z) = \int_{\text{Galaxy}} dn(\rho, \phi, z, \rho_s, \phi_s, z_s). \quad (5)$$

and the emissivity of 1809 keV photons at point (ρ, ϕ, z) can then be written as $\epsilon(\rho, \phi, z) = N(\rho, \phi, z)/\tau_o$.

The observed gamma-ray flux from Galactic coordinates (l, b) is then just the integral along the line-of-sight

$$\frac{dF}{dA dt d\Omega}(l, b) = \int_0^\infty \frac{\epsilon(l, b, r)}{4\pi r^2} r^2 dr = \frac{1}{4\pi} \int_0^\infty \epsilon(l, b, r) dr, \quad (6)$$

where r is the radial coordinate along the line-of-sight and

$$\rho(l, b, r) = \sqrt{\rho_\odot^2 + r^2 \cos^2 b - 2r\rho_\odot \cos b \sin l} \quad (7a)$$

$$z(b, r) = r \sin b. \quad (7b)$$

There is no attenuation term in equation (6) since the Galaxy is transparent to 1809 keV radiation. Thus this model has 7 parameters: ϵ_o , α , β , z_o , ρ_\odot , z_\odot , and v_o , all of which are constrained by observations.

We have used the approximation in this model that the dust grain motion is convective, not diffusive. We have previously shown that dust grains must interact with shocks in the ISM every 100 - 200 pc along their trajectory in order to maintain a velocity of $\sim 500 \text{ km s}^{-1}$ (Sturmer & Naya 1999). The distance a dust grain must travel in the ISM for collisions with gas to appreciably change the grain direction (and thus the energy) will be similar to this distance if there is to be an equilibrium between shock acceleration and collisional energy losses. The mean distance a grain with velocity v_o will travel in time t is given by $L = \sqrt{\lambda v_o t}$. Using 100 - 200 pc for the mean-free-path λ , the diffusion length in the 10^6 year lifetime of the ^{26}Al is 226 - 320 pc for $v_o = 500 \text{ km s}^{-1}$ as compared to the 500 pc distance along the particle path. We can then define a mean grain velocity, $\langle v \rangle \equiv L(\tau_o)/\tau_o = \sqrt{\lambda v_o/\tau_o} = 226 - 320 \text{ km s}^{-1}$. This diffusion length and mean velocity should be considered a lower limit as the dust grain mean-free-path will grow as they move farther from the Galactic plane. In the next section we discuss the results of this model for grains with velocities of 100, 275, 500, and 1000 km s^{-1} .

3. Results

In our simulations we have set all parameters to those values given in Section 2 except for varying the particle velocity from 100 km s^{-1} to 1000 km s^{-1} to illustrate how the results change with the dust grain velocity. We chose to include results for $v_o = 275 \text{ km s}^{-1} \approx \langle v \rangle$ to approximate diffusive motion of the grains with a true space velocity of 500 km s^{-1} . In Figure 2 we show the 1809 keV emissivity as a function of Galacto-centric radius ρ and height z calculated from equation (5). These plots show a broad peak near $\rho = 5 \text{ kpc}$ that mimics the ^{26}Al production function. We find, as expected, that as the grain velocity is increased, the emissivity in the plane decreases while it increases at larger z and the "hole" in the production function at the Galactic Center becomes less evident.

We used these results to calculate skymaps of the 1809 keV emission in the range $-90^\circ \leq l \leq 90^\circ$ and $-30^\circ \leq b \leq 30^\circ$. These maps were then convolved with a 3.8° FWHM Gaussian to approximate the effect of the COMPTEL point spread function (PSF) on the image. In Figure 3 we show normalized contour plots for the convolved and unconvolved emission maps for models with $v_o = 275$ and 500 km s^{-1} to illustrate the degree to which our approximate COMPTEL PSF alters the skymap. The effect of the broad PSF on the contour plots is significant. We find that much of the emission in the Galactic plane is “transported” to higher latitudes. We wish compare these skymaps to the COMPTEL data.

Knödlseider et al. (1999a) compared several algorithms for performing imaging analysis of COMPTEL 1809 keV data, including maximum entropy (ME), Richardson-Lucy (RL), and multiresolution regularized expectation maximization (MREM). ME reconstructions were very sensitive to statistical noise and tended to produce artificial hot spots that may be indistinguishable from real point sources. MREM analysis produced a smoother map but at the expense of suppressing weak features. They found that MREM yielded a latitude profile (averaged over $-90^\circ \leq l \leq 90^\circ$) with a $\text{FWHM} = 7.5^\circ$ while the RL and ME methods yielded somewhat wider profiles with widths $\sim 8^\circ$. We have used our convolved model skymaps to generate similarly averaged latitude profiles for the emission. In Figure 4 we compare the model profiles with the MREM, RL, and ME profiles of Knödlseider et al. (1999a). This comparison consisted of renormalizing the model profiles so that the peak flux for a given model matched the peak flux of a particular reconstructed map. We have also shifted the model profiles slightly in b so that they were approximately centered on the data. It should be noted that these are not mathematical fits to the data using χ^2 or any other statistic. They are only qualitative comparisons to the data since our purpose in this paper is ascertain whether high-velocity ^{26}Al is consistent with the observed spatial distribution of 1809 keV emission and not to deduce the exact parameters of this somewhat simplified model that best fit the data.

The three data reconstruction methods produce significantly different profiles. There is more than a factor of 2 difference between the peak flux in the MREM profile and the ME profile. The fluxes in the wings of the RL and ME profiles are similar but the MREM profile has significantly less emission at $|b| > 5^\circ$. We find that the MREM reconstruction is poorly fit by all models. This reconstructed map has the brightest emission in the Galactic plane while having the dimmest emission at high latitudes. The $v_o = 1000 \text{ km s}^{-1}$ profile fits the data well for $-2.5^\circ \lesssim b \lesssim 2.5^\circ$ but it overproduces emission at higher latitudes by a large margin. The other models produce less high latitude emission but do not match the lower latitude emission. The RL map is best fit by the model with $v_o = 500 \text{ km s}^{-1}$. The 275 km s^{-1} emission profile is significantly narrower than the core of the COMPTEL profile but has the correct emission level at higher latitudes while the 1000 km s^{-1} emission profile fits the COMPTEL data reasonably well in the latitude range $-3^\circ \lesssim b \lesssim 3^\circ$ but the emission is too bright at higher latitudes. The ME map is best fit by the 1000 km s^{-1} model. This model fits the data reasonably well in the region $-4^\circ \lesssim b \lesssim 4^\circ$ with a small excess at higher latitudes. The higher latitude emission is best fit by the 500 km s^{-1} emission. Thus we find that while the model with $v_o = 1000 \text{ km s}^{-1}$ can fit all the reconstructed maps at the lowest latitudes, the models with $v_o = 275$ and 500 km s^{-1} fit the RL and ME reconstructed data for $|b| \gtrsim 5^\circ$ but tend to underpredict the lower latitude emission. Considering the simplicity of the model, including mono-energetic dust grains, the results are quite good. Thus we find that the spatial distribution of the 1809 keV emission measured by COMPTEL is not in conflict with the GRIS measurement of high velocity ^{26}Al .

One way to possibly improve the fit of the model to the data is to use a somewhat larger scale height, z_o , for the production function coupled with grain velocity $\sim 275 - 500 \text{ km s}^{-1}$. The larger scale height will broaden the lowest latitude emission while the moderate velocity (in the context of this paper) will act to keep the higher latitude emission at a lower level. A somewhat larger scale height can be justified given that the 90 pc supernova scale that

we use is in our calculations is really a lower limit taken from the scale height of massive stars. There is also some evidence that massive stars exist (and thus supernovae must occur) at significant distances above the plane of our Galaxy. As we have previously stated, Knodlseder (1999b) found that the 53 GHz free-free emission map obtained by the *COBE* DMR (Bennett et al. 1992) produced the best fit to the COMPTEL 1809 keV map when comparing 31 emission maps with energies from radio through gamma ray. This free-free emission is a tracer of ionized gas and thus the O and B stars in the Galaxy. The ionized hydrogen gas in our Galaxy can be described using four components, compact and diffuse H II regions which are well confined to the disk, as well as two low-density diffuse components with significantly larger scale heights (Lockman, Pisano, & Howard 1996; Taylor & Cordes 1993). The diffuse and compact H II regions have similar vertical distributions with a FWHM ≈ 50 pc (Lockman et al. 1996). The two diffuse components have vastly different distributions. The higher density component ($n = 0.1 \text{ cm}^{-3}$) dominates the inner Galaxy and has a FWHM $\simeq 260$ pc while the lower density ($n = 0.019 \text{ cm}^{-3}$) outer Galaxy component has a much larger FWHM $\simeq 1540$ pc (Taylor & Cordes 1993). The origin of this low density component is poorly understood (Lockman et al. 1996).

The model normalization calculated for the fits in Figure 4 can be used to calculate the ^{26}Al mass in the Galaxy which we list in Table 1. Those models that best fit the data produce $\sim 1.5 - 2 M_{\odot}$ of ^{26}Al in the Galaxy given the $\sim 1.04 \times 10^6$ year mean lifetime. These masses compare favorably with those calculated from observations and theoretical models. Mahoney et al. (1984) calculated the Galactic mass of ^{26}Al to be $\sim 3 M_{\odot}$. Knodlseder (1997) calculated the mass to be $1.6 - 2.2 M_{\odot}$ using exponential disk models. Much smaller values for the Galactic mass result if much of the ^{26}Al is produced locally ($\lesssim 1$ kpc of the Sun). Diehl et al. (1995) find that if there are 5-10 local sources each with a flux of 3×10^{-5} photons $\text{cm}^{-2} \text{ s}^{-1}$, the Galactic mass of ^{26}Al would be reduced to $\sim 1 M_{\odot}$. Timmes et al. (1995) have calculated the Galactic production rate and mass of ^{26}Al using

models for the production of ^{26}Al in Type II SNe as function of progenitor mass as well as stellar mass and birth-rate functions. They found that Type II SNe should produce $2.0 \pm 1.0 M_{\odot} \text{ Myr}^{-1}$ yielding a Galactic mass of ^{26}Al of $2.2 \pm 1.1 M_{\odot}$ in agreement with our estimate. We do not suggest this is proof for a Type II SN origin for the ^{26}Al . The required $2 M_{\odot}$ of ^{26}Al can in principle be produced by any of the sources mentioned in Section 1 (see e.g. Diehl & Timmes 1997) and the uncertainties in the true 3-dimensional distribution of the ^{26}Al make it difficult to rule out any type of sources.

The SPI germanium imaging spectrometer on *INTEGRAL* may help resolve the question of the origin of ^{26}Al in our Galaxy (see e.g. Vedrenne et al. 1999). One of the prime objectives of SPI is to map the Galactic Center and the Galactic plane at both 511 keV and 1809 keV. SPI combines an energy resolution at 1809 keV that should be at least as good as the 3.4 keV resolution of GRIS with a 2.0° angular resolution which is superior to COMPTEL. The SPI detector array will also have roughly twice the area and volume as the GRIS array. Thus the superior quality and quantity of the data should allow for SPI to confirm or contradict the GRIS line-width results. The good angular resolution and the high sensitivity of SPI to line emission should allow for the determination of line width as a function of position on the sky. This used in conjunction with the overall map of the emission may allow for a determination of the major source(s) of the ^{26}Al .

REFERENCES

- Arnett, W.D. 1977, *Ann. N.Y. Acad. Sci.*, 302, 90
- Bahcall, J.N., & Soneira, R.M. 1980, *ApJS*, 44, 73
- Bennett, C.L., et al. 1992, *ApJ*, 396, L7
- Case, G.L., & Bhattacharya, D. 1998, *ApJ*, 504, 761
- Chen, W., et al. 1997, in *Proc. 2d INTEGRAL Workshop, The Transparent Universe*, ed. C. Winkler, T. J.-L. Courvoisier, & Ph. Durouchoux (ESA SP-382;Noordwijk:ESA), 105
- Clayton, D.D. 1982, *QJRAS*, 23, 174
- Clayton, D.D., & Leising, M.D. 1987, *Phys. Rep.*, 144, 1
- Diehl, R., & Timmes, F.X. 1997, in *AIP Conf. Proc. 410, Proc. 4th Compton Symp., Part 1*, ed. C. D. Dermer, M. S. Strickman, & J. D. Kurfess (New York:AIP), 218
- Diehl, R. et al. 1995, *A&A*, 298, 445
- Diehl, R. et al. 1997, in *AIP Conf. Proc. 410, Proc. 4th Compton Symp., Part 1*, ed. C. D. Dermer, M. S. Strickman, & J. D. Kurfess (New York:AIP), 1114
- Drain, B.T., & Salpeter, E.E. 1979, *ApJ*, 231, 77
- Dwek, E. 1988, *ApJ*, 329, 814
- Dwek, E., et al. 1983, *ApJ*, 274, 168
- Dwek, E., et al. 1992, *ApJ*, 389, L21
- Ellison, D.C., Drury, L. O'C., & Meyer, J.-P. 1997, *ApJ*, 487, 197
- Ferrière, K. 1993, *ApJ*, 409, 248
- Knödlseher, J. 1997, Ph.D. Thesis, l'Universite Paul Sabatier de Toulouse

- Knödlseeder, J. et al. 1999a, *A&A*, 345, 813
- Knödlseeder, J. et al. 1999b, *A&A*, 344, 68
- Lockman, F.J., Pisano, D.J., & Howard, G.J. 1996, *ApJ*, 472, 173
- Mahoney, W.A., Ling, J.C., Wheaton, W.A., & Jacobson, A.S. 1984, *ApJ*, 286, 578
- Miller, G.E., & Scalo, J.M. 1979, *ApJS*, 41, 513
- Naya, J.E., et al. 1996, *Nature*, 384, 44
- Oberlack, U. 1997, Ph.D. Thesis, Technische Universität München
- Prantzos, N. & Diehl, R. 1996, *Phys. Rep.*, 267, 1
- Ramaty, R., & Lingenfelter, R.E. 1977, *ApJ*, 213, L5
- Share, G.H., Kinzer, R.L., Kurfess, J.D., Forrest, D.J., Chupp, E.L., Rieger, E. 1985, *ApJ*, 292, L61
- Stecker, F.W., & Jones, F. 1977, *ApJ*, 217, 843
- Sturmer, S.J., & Naya, J.E. 1999, *ApJ*, 526, 200
- Taylor, J.H., & Cordes, J.M. 1993, *ApJ*, 411, 674
- Vedrenne, G., et al. 1999, *Astrophys. Lett. Comm.*, 39, 325

Table 1: Model Galactic Mass of ^{26}Al

v_0 (km s $^{-1}$)	Reconstruction Method	ϵ_0 (10^{-25} cm $^{-3}$ s $^{-1}$)	Mass of ^{26}Al (M_\odot)
100	MREM	8.95	1.82
100	RL	6.25	1.27
100	ME	4.28	0.87
275	MREM	11.0	2.23
275	RL	7.68	1.56
275	ME	5.26	1.07
500	MREM	13.6	2.76
500	RL	9.48	1.93
500	ME	6.49	1.32
1000	MREM	18.8	3.82
1000	RL	13.1	2.66
1000	ME	8.98	1.82

Figure Captions

Figure 1: Plot of the SNR surface density function given in Equation 5. The parameter values are those used throughout our models: $\rho_{\odot} = 8.5$ kpc, $\alpha = 2.0$, and $\beta = 3.53$. The peak between 4.5 and 5.0 kpc leads to the peak in the emissivity plots in Figure 2 and the peaks seen in the emission contours in Figures 3a-d.

Figure 2: Here we show the 1809 keV emissivity as a function of Galacto-centric radius for $v_{\circ} = 100, 275, 500,$ and 1000 km s⁻¹ and $z = 0$ (solid), 250 (dashed), 500 (dotted), and 1000 pc (dot-dot-dot-dashed). We have chosen $\epsilon_{\circ} = 1.0 \times 10^{-24}$ cm⁻³ s⁻¹ (see Table 1). Note that as the dust grain velocity increases the emissivity decreases at small z but increases at large z , as expected.

Figure 3: Here we show contour plots of the observed 1809 keV flux for the models with $v_{\circ} = 275$ km s⁻¹ and 500 km s⁻¹. We show contour plots for maps that have been convolved with the 3.8° FWHM PSF (3b and 3d) and those that have not (3a and 3c). The plots for each velocity have been normalized by dividing by the peak flux in the unconvolved map. This normalization shows the decrease in the observed peak flux that results from having a large instrumental PSF. The peaks seen at $\sim \pm 20^{\circ}$ result from the peak in the ²⁶Al production function at 4.8 kpc.

Figure 4: Here we compare longitude-averaged ($-90 \leq l \leq 90$) latitude profiles for the multiresolution regularized expectation maximization (MREM) (a), Richardson-Lucy (RL) (b), and maximum entropy (ME) (c) reconstructed COMPTEL 1809 keV emission maps (solid) with our model with $v_{\circ} = 100$ km s⁻¹ (dotted), 275 km s⁻¹ (short dashed), 500 km s⁻¹ (dot-dashed), and 1000 km s⁻¹ (long dashed). We have normalized the model profiles such that the peak fluxes equal those for the data. We have also slightly offset the flux peak to negative values of b to center the model profiles on the data. Note that none of the models can reproduce the contrast between the Galactic plane and the higher latitudes seen

in the MREM reconstruction. The 1000 km s^{-1} model best fits the data at lowest latitudes while the 275 km s^{-1} and 500 km s^{-1} models best fit the emissio for $|b| > 5^\circ$.

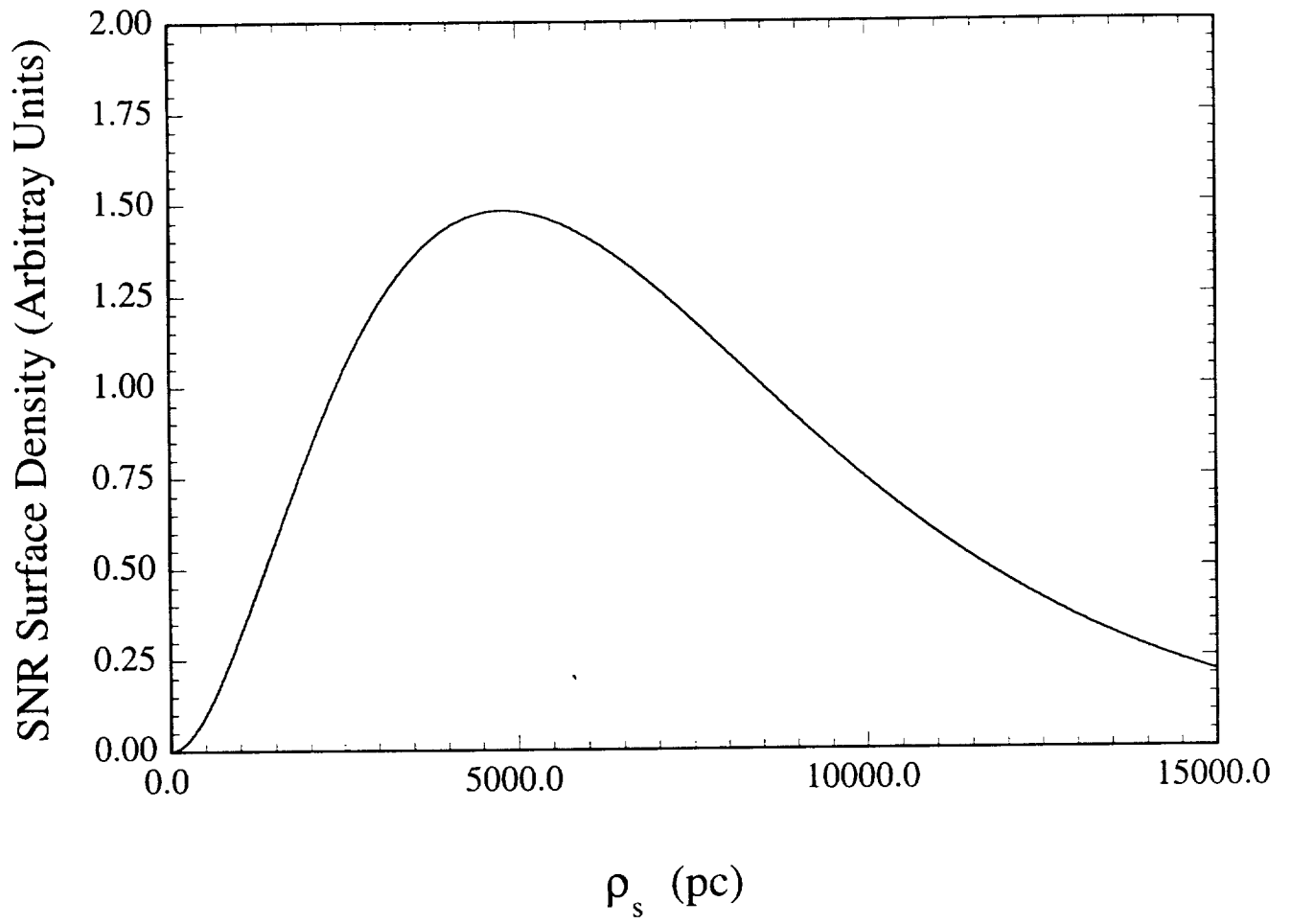


Figure 1

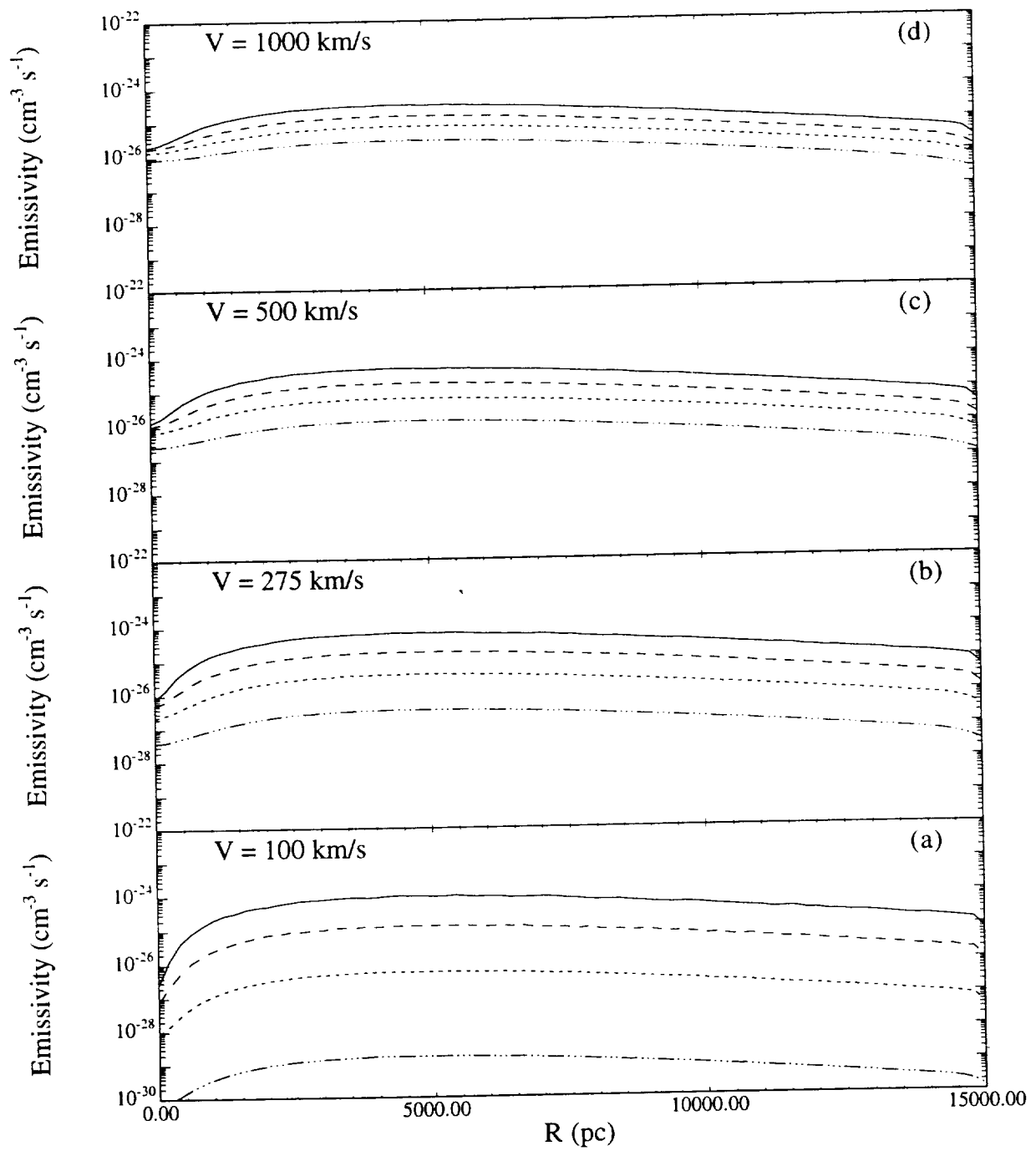


Figure 2

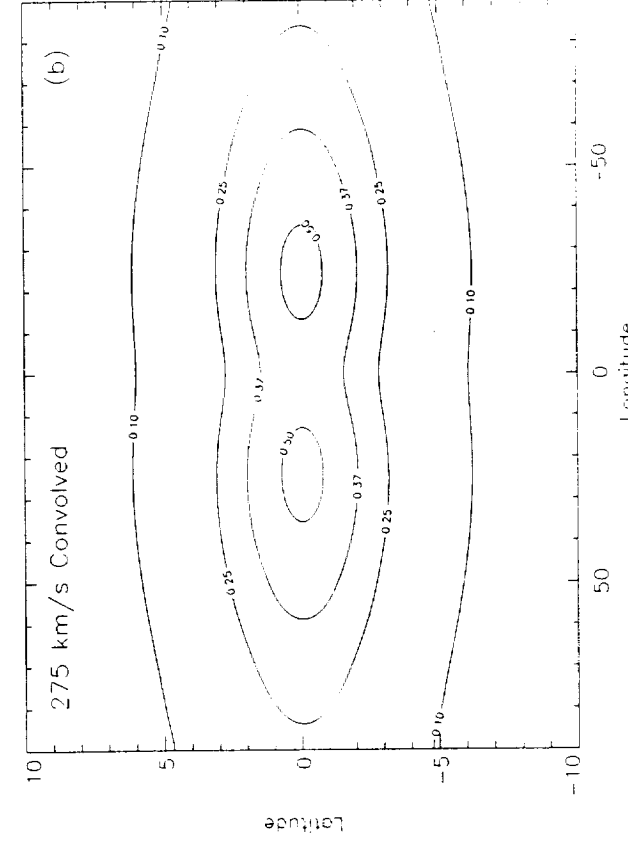
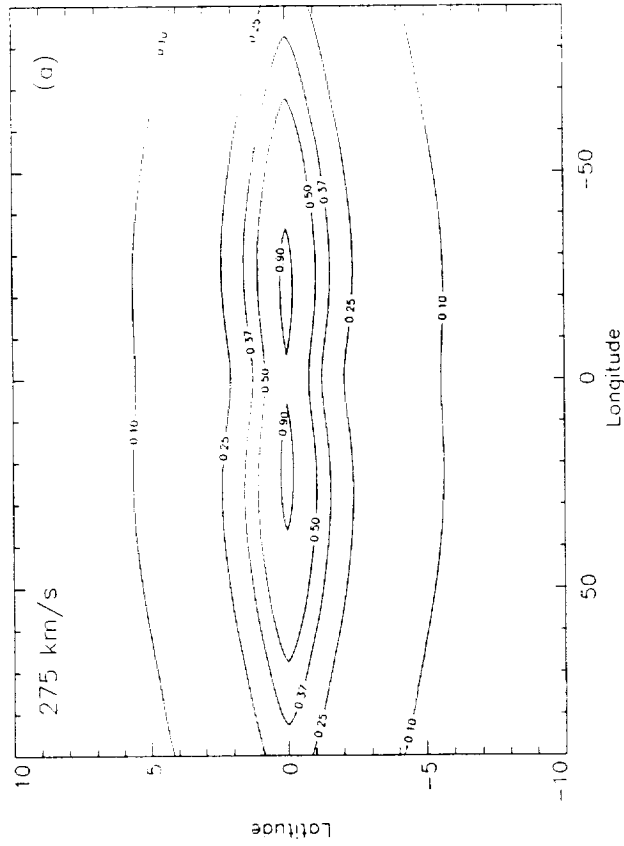
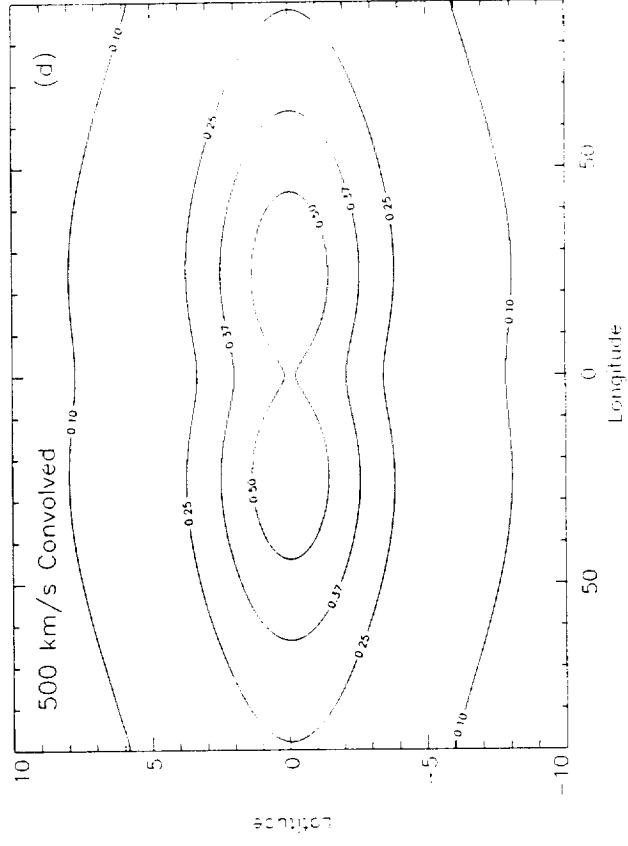
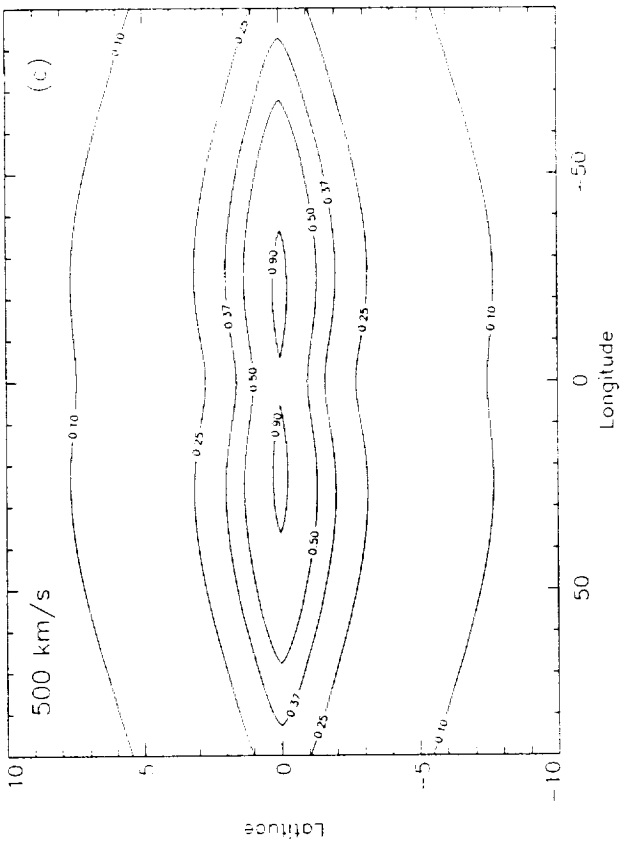


Figure 3

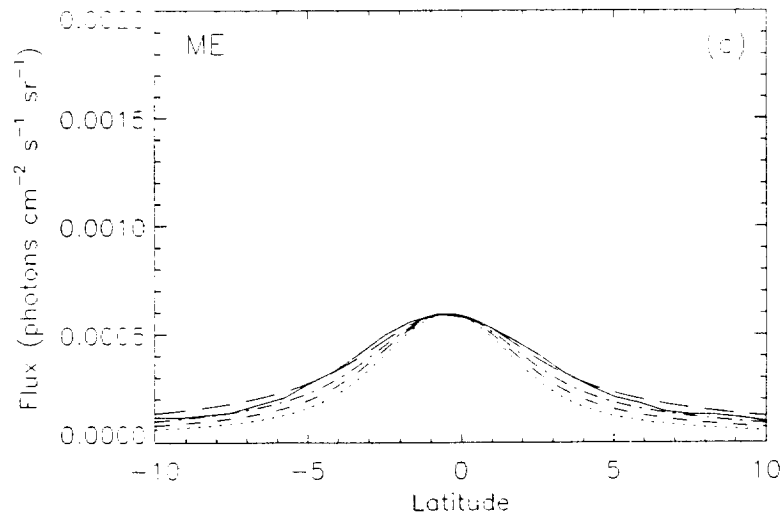
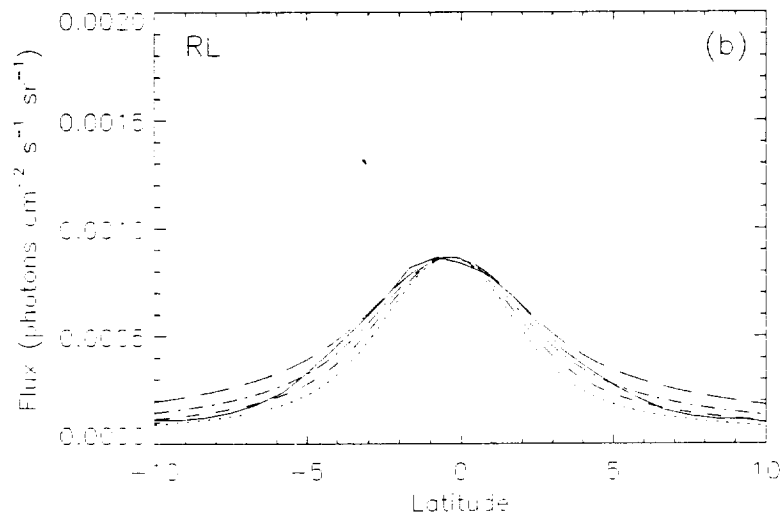
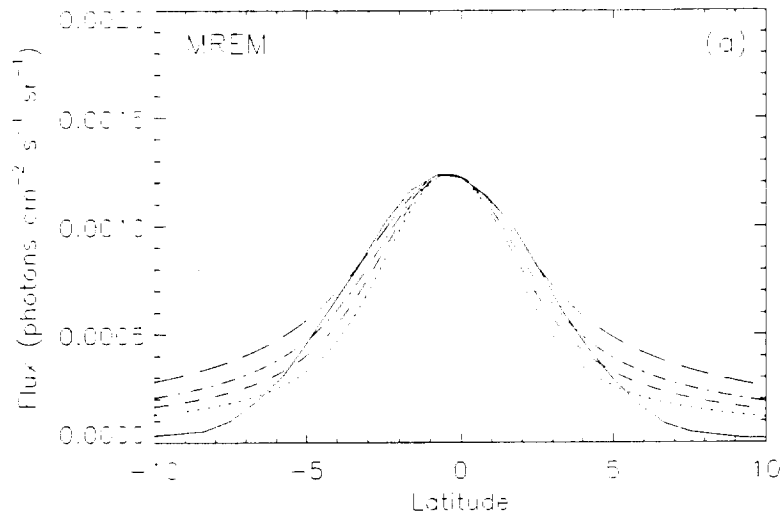


Figure 4